JOURNAL OF SOLID STATE CHEMISTRY 79, 238–249 (1989)

Atmospheric Degradation of $YBa_2Cu_3O_7$: A Study by Infrared Reflectance, Raman Scattering, and X-Ray Photoelectron Spectroscopy

R. G. EGDELL, W. R. FLAVELL,* AND P. C. HOLLAMBY

Centre for High Temperature Superconductivity, Department of Chemistry, Imperial College, London SW7 2AZ, United Kingdom

Received August 25, 1988; in revised form December 16, 1988

Infrared reflectance spectroscopy, Raman scattering, and X-ray photoelectron spectroscopy have been used to study the atmospheric degradation of $YBa_2Cu_3O_{7-\delta}$. The degradation reaction: $2YBa_2Cu_3O_7 + 3CO_2 \rightarrow Y_2BaCuO_5 + 5CuO + 3BaCO_3 + 0.5O_2$ is strongly catalyzed by water vapor, and carbonate species build up in a matter of hours on an IR depth scale at room temperature in water vapor saturated air. The reaction is rapid even for reduced samples ($x = 1.0$) containing no Cu(III).

1. Introduction

Following the discovery of high-temperature oxide superconductors (*1–3*), there has been a growing interest in the surface and interfacial properties of the new materials. In polycrystalline oxides transport properties are undoubtedly determined to a large extent by intergrain contact. For $YBa_2Cu_3O_7$ in particular it is now fairly well established that critical current densities achievable in polycrystalline materials are limited by the weak links provided by grain boundaries (*4, 5*). There is, however, some controversy as to the role of impurities in limiting the intergrain superconductivity (*6*). Moreover contact to superconducting samples must be made through the external surface. Thus it is necessary to study surface and grain boundary composition and electronic structure in relation to transport properties.

The new "high-temperature" superconductors in common with other oxides may react with atmospheric water or CO_2 to give hydroxides or carbonates. Many workers who have dealt with $YBa_2Cu_3O_7$ have some experience of samples "going off" as a result of storage (*7*), presumably due to reaction with air. Aside from the fact that atmospheric degradation may pose major problems in the technological application of the new oxide superconductor, it must also be recognized that many of the experimental techniques directed toward elucidating the mechanism of the superconductivity in the oxides look at sample surfaces with varying degrees of surface specificity and thus can be influenced by reaction with atmosphere to give contaminant overlayers. For example, in tunneling experiments directed toward measurement of the super-

* To whom correspondence should be addressed.
0022-4596/89 $3.00

conducting gap, at least three groups (*8–10*) have found that to obtain reproducible tunnel currents it is necessary to drive tunnel tips into the sample surface through an insulating surface layer. In Raman spectroscopy, a favored technique for looking at phonon structure, the signal from the metallic phase $YBa_2Cu_3O_7$ is much weaker (*11*) than from the nonmetallic phase Y_2BaCuO_5 that may be formed by reaction with air (see below). Thus it is crucial not to confuse Raman signals from the $YBa_2Cu_3O_7$ "123" phase with those from degradation products. Several Raman studies nominally on $YBa_2Cu_3O_7$ have yielded spectra with peaks attributable to Y_2BaCuO_5 [e.g., Ref. (*12*)]. Studies of superconducting phases by XPS and photoemission are particularly surface sensitive with effective sampling depths of around 5–20 Å. Much of fundamental interest about band structure, correlation, etc., is to be learned, but before this can be done it is crucial to appreciate the role of contamination. It is a recurring observation in the literature that it is difficult to prepare $YBa_2Cu_3O_7$ surfaces free of carbon in the surface region (*13*).

In a series of simple but elegant experiments, Yan *et al.* (*14*) demonstrated that $YBa_2Cu_3O_7$ decomposes rapidly when immersed in liquid water or exposed to water vapor at 85°C. X-ray diffraction studies showed the presence of $BaCO_3$, CuO, and the green phase Y_2BaCuO_5 in the resulting solid product and O_2 was liberated according to the equation:

$$3H_2O + 2YBa_2Cu_3O_7 \rightarrow Y_2BaCuO_5 + 5CuO + 3Ba(OH)_2 + 1/2O_2. \quad (1)$$

$Ba(OH)_2$ reacts rapidly with atmospheric CO_2 to give carbonate species:

$$3CO_2 + 3Ba(OH)_2 \rightarrow 3BaCO_3 + 3H_2O. \quad (2)$$

Thus water simply acts as a catalyst for the formation of carbonate species. Similar patterns of reactivity were found by Nakada *et al.* (*15*), while Kitazawa and co-workers (*16*) showed that electrochemical corrosion currents associated with the decomposition reaction can create resistivity anomalies around room temperature. In more fundamental studies, Johnson and co-workers showed that water reacts with $YBa_2Cu_3O_7$ under UHV exposures of the order of several Langmuirs to give hydroxyl species (*17*). Reaction of $YBa_2Cu_3O_7$ with CO_2 has not yet been studied in a UHV system, but Madey and co-workers found that CO_2 and H_2O have unit sticking coefficients for interaction with $La_{2-x}Sr_xCuO_4$ to give surface carbonate and hydroxyl anions (*18*).

We have been concerned with the study of atmospheric degradation of the 123 superconductor and carbonate buildup under conditions approximating more closely to those encountered in the normal storage and use of the material than in the water immersion and *in situ* UHV experiments referred to above. To this end we have used three spectroscopic techniques of differing surface sensitivities. These are (i) IR reflectance spectroscopy where the probing depth for dielectric overlayers can be equated roughly with the wavelength of the IR radiation, i.e., 10^5 Å or 10 μm at 1000 cm^{-1}; (ii) Raman spectroscopy where surface sensitivity depends on penetration of the visible laser radiation used to excite the spectra (if this is of the order of the wavelength of the incident radiation, then we have ~0.5 μm for the Ar 488 nm blue line); and (iii) X-ray photoelectron spectroscopy where the effective probing depth depends on the inelastic pathlength of the photoelectrons. This is of the order of 20 Å, i.e., 0.002 μm. The thin contaminant layers probed by XPS would probably be of little interest in the study of conventional superconductors where coherence lengths are much larger than those in the new materials (*19, 20*). However, with coherence lengths of only a few tens of Ångstroms in the oxide materials, XPS surface studies assume an

important role. Our studies are also motivated by our own extensive surface science program and our consequent need to establish handling and cleaning procedures compatible with surface experiments.

2. Experimental

The 123 material used in the present work was prepared by the usual solid-state reaction as described previously (*6*) using high-purity $BaCO_3$, Y_2O_3, and CuO. The aggregate from the initial firing was ground finely in an agate mortar and pressed into 13-mm-diameter pellets between tungsten carbide dies. Note that prolonged high-temperature heating of the resulting pellets at 950°C was employed to ensure complete reaction of the starting materials, followed by extended anneals at 400°C to allow complete oxygen uptake. Pellets prepared in this way displayed metallic conductivity at room temperature and underwent a sharp resistive transition to a superconducting state with zero resistance at 91 K. They gave X-ray powder patterns characteristic of the orthorhombic 123 phase free of signals due to starting materials or contaminant phases such as Y_2BaCuO_5 or $BaCuO_2$. The pellets displayed typical metallic reflectances with up to 65% reflectivity at 400 cm^{-1} (Fig. 1, curve m). Conversion to a nonmetallic tetragonal phase was effected through a firing cycle in flowing nitrogen similar to that usually used for oxygen uptake. After the nitrogen annealing the pellets were nonmetallic at room temperature and gave pronounced Restrahl phonon features in infrared reflectance typical of the nonmetallic phase (*21*) (Fig. 1, curve n). Pellets of the green phase Y_2BaCuO_5 and of CuO, Y_2O_3, and CuO were prepared for comparative study.

Degradation of pellets was studied only at the ambient room temperature of a large teaching laboratory (20°C < T < 25°C). One set of pellets was exposed to an ambient London atmosphere over a period of 100 days starting in January 1988. Others were stored in one of four large dessicators loaded to provide controlled partial pressures of water vapor. The loadings were: distilled H_2O ($P(H_2O)$ = 21.2 mm Hg); 8% (by weight) H_2SO_4/H_2O ($P(H_2O)$ = 17.0 mm Hg); 22% H_2SO_4/H_2O ($P(H_2O)$ = 15.4 mm Hg); $CuSO_4 \cdot 5H_2O/CuSO_4 \cdot 3H_2O$ ($P(H_2O)$ = 7.5 mm Hg). In each case $P(CO_2)$ was maintained at its normal atmospheric value by regular opening of dessicators for IR reflectance studies. A final set of sample pellets were kept for periods of time up to 1 year in plastic stoppered glass sample bottles of the sort routinely used for sample storage in programs of solid-state synthetic chemistry.

IR specular reflectance spectra were measured at 16 cm^{-1} resolution using a simple two-mirror reflectance attachment mounted in a Mattson Alpha-Centauri interferometer equipped with a KBr beamsplitter and DTGS pyroelectric detector. Reflectance was normalized to that of an aluminium mirror.

Raman spectra were excited with the 488-nm (blue) line of an Ar^+ laser (Coherent UK Ltd) and measured with a Spex Ramalog double-grating monochromator. Multiple scans were accumulated using a Spex Datamate data handling system.

Al$K\alpha$ X-ray photoelectron spectra were measured in a VG ESCALAB Mark II spectrometer with the analyzer resolution set at 0.4 eV. In addition to the analysis chamber (base pressure 5 × 10^{-11} Torr), the spectrometer has a fast entry lock and preparation chamber. Samples were mounted on platinum stubs and secured with platinum clips. Care was taken not to allow the clips to protrude onto the sample surface. Samples were examined both in their native state as inserted into the spectrometer after being stored under a variety of conditions and after cleaning *in situ* inside the spectrometer. Cleaning was ef-

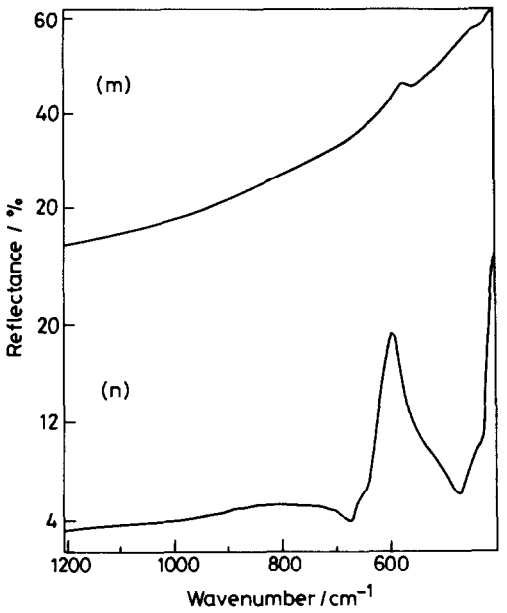

FIG. 1. Infrared reflectance spectra of ceramic pellets of $YBa_2Cu_3O_{7-x}$ in both metallic (m) and nonmetallic (n) phases.

fected by filling the preparation chamber with pure oxygen and heating the platinum stub by coupling to the radiofrequency field provided by a water-cooled copper work-coil connected through a Leybold Heraeus RF feedthrough to a Radyne 1.5-kW 400-kHz power supply. The cleaning cycle was designed to mimic the conditions of sample preparation and typically involved heating to around 600–700°C for 1 hr, followed by cooling to 400°C over a period of several hours. After switching off the RF power, samples were allowed to cool to room temperature in oxygen, before evacuation of the preparation chamber. XPS were typically recorded within 1 hr of sample cleaning.

3. Results and Discussion

Figure 1 shows IR reflectance spectra in the range 1200–400 cm^{-1} for metallic and nonmetallic phases of $YBa_2Cu_3O_{7-\delta}$. The spectrum of the metallic phase is largely structureless and shows the expected high metallic reflectance, which rises toward 100% as $\hbar\omega \rightarrow 0$. Features due to the lattice phonons are largely screened out by the carriers present. After nitrogen annealing, the spectrum obtained was typical of a nonmetallic metal oxide and showed low reflectance with strong Restrahl phonon features beyond 700 cm^{-1}. The strong band at ~600 cm^{-1} has been attributed to the in plane Cu–O E_u stretch (ω_{TO} = 593 cm^{-1}), while the shoulder at ~650 cm^{-1} is assigned to the A_u Cu–O chain mode parallel to the c-axis (ω_{TO} = 648 cm^{-1}) (*21*).

Figure 2 shows the reflectance spectra of the metallic phase $YBa_2Cu_3O_7$ in the as-pre-

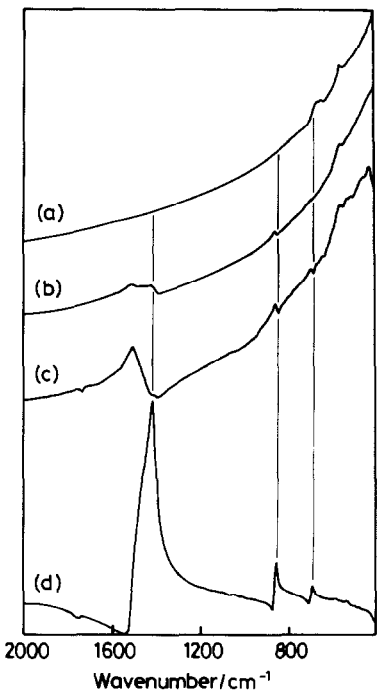

FIG. 2. IR reflectance spectra of polycrystalline $YBa_2Cu_3O_7$ (a) as prepared (10–60%); (b) after exposure to water vapor saturated air at 23°C for 21 hr (8–49%); (c) as (b) but after 92 hr (1–7%); (d) IR reflectance of $BaCO_3$ (4–23%). Values in parentheses refer to the reflectance for each trace at 2000 and 400 cm^{-1}, respectively.

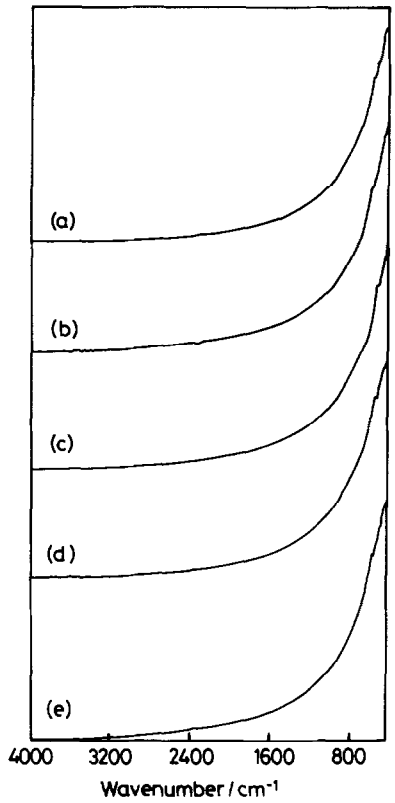

FIG. 3. IR reflectance of polycrystalline $YBa_2Cu_3O_7$ exposed to air containing water vapor at partial pressure of 7.5 mm Hg (a) as prepared (3–29%), (b) after 25 hr (3–29%), (c) after 97 hr (3–29%), (d) after 168 hr (3–31%), (e) after 240 hr (3–31%). Values in parentheses refer to the reflectance for each trace at 4000 and 400 cm^{-1}, respectively.

pared state, and after exposure to water vapor saturated air for different periods of time. These are compared with the IR reflectance of $BaCO_3$ over the same frequency range (Fig. 2d), which shows three very strong Restrahl bands associated with the internal vibrations of the CO_3^{2-} anion. These are assigned to the B_{1u}, B_{1u}, and B_{2u} modes at 693, 855, and 1445 cm^{-1}, respectively (*22*). It can be seen that features which may be associated with the production of $BaCO_3$ appear in the spectra of $Y_2BaCu_3O_7$ on exposure to water vapor, and these features increase in intensity as exposure continues. Experiments revealed that the other starting materials, CuO and Y_2O_3 and the green phase YBa_2CuO_5, show no features in the range above ~600 cm^{-1}. It is noticeable that the new features introduced by carbonate buildup correspond to dips in reflectivity at positions corresponding to the band maxima of the internal CO_3^{2-} anion modes. We note that the effect of a dielectric layer on a metallic substrate is to produce dips in the IR reflectivity at the LO phonon frequencies of the overlayer (*19*). In this case, the separation between the LO and TO phonon frequencies of the internal CO_3^{2-} modes is small (*23*); for example, for the B_{1u} mode at 855 cm^{-1}, the LO and TO frequencies are estimated at 875.5 and 852 cm^{-1}, respectively (*23*). Thus we would anticipate in this case that the production of an insulating $BaCO_3$ layer on top of the metallic 123 phase would result in a spectrum showing dips in reflectivity at positions approximating those of the internal CO_3^{2-} anion band maxima, as is observed.

Figure 3 shows a series of reflectance spectra for $YBa_2Cu_3O_7$ exposed to air containing water vapor at a partial pressure of 7.5 mm Hg. It can be seen that the rate of carbonate buildup relative to that for saturated water vapor is greatly diminished for $P(H_2O)$ = 7.5 mm Hg, as virtually no carbonate features are visible even after exposure times of 240 hr. Small features in the ranges 2400–2300 and 3700–3300 cm^{-1} are due to atmospheric CO_2 and H_2O, respectively, and arise from imperfect cancellation between background and sample scans due to fluctuations in the environment inside the spectrometer.

The changes in the spectra are quantified in Fig. 4, which shows in the top panel the reflectance at 400 cm^{-1} (normalized to the initial reflectance of the as-prepared pellet at 400 cm^{-1}) as a function of time, for water vapor at two different partial pressures. In the case of saturated water vapor, this decreases rapidly, as the sample surface de-

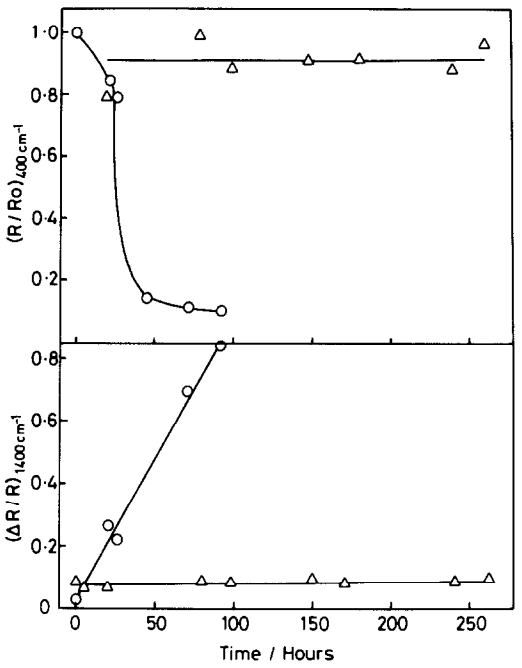

FIG. 4. Variation of reflectance at 400 cm^{-1} and reflectance change across the carbonate Restrahl band at 1400 cm^{-1} for polycrystalline $YBa_2Cu_3O_7$ as a function of time. Circles, exposed to air containing water vapor at 21.2 mm Hg; triangles, exposed to air containing water vapor at 7.5 mm Hg.

grades and becomes rougher. At $P(H_2O)$ = 7.5 mm Hg, R/R_0 remains approximately constant. In the lower panel of the figure, the reflectance drop, ΔR, across the CO_3^{2-} Restrahl band at ~1400 cm^{-1} is plotted and normalized to the mean reflectance, R, across this band. (This is achieved by subtraction of a linear sloping background from the initial spectra.) Again, we observe a marked difference between $P(H_2O)$ = 21.2 mm Hg and $P(H_2O)$ = 7.5 mm Hg. In the case of the latter, $\Delta R/R$ remains constant, while under saturated water vapor, there is a linear increase in $\Delta R/R$, concomitant with carbonate buildup.

The results appear to show that the reaction of the surfaces of the $YBa_2Cu_3O_7$ pellets with atmospheric CO_2 is catalyzed by the presence of water vapor, but that the reaction shows a very nonlinear dependence on $P(H_2O)$. One consequence of this is that the rate of degradation of the 123 phase exposed to air in a temperate climate of moderate humidity is rather slow. This is illustrated in Fig. 5, which shows IR reflectance of polycrystalline $YBa_2Cu_3O_7$ pellets exposed to the ambient atmosphere in London during the period January–April 1988. During this time the atmospheric water vapor partial pressure was in the range 6.75–8.25 mm Hg. It can be seen that even after 2400 hr exposure, no appreciable degradation is apparent on the IR depth scale. Again, features in the range 2400–2300 cm^{-1} are due to fluctuations in the atmospheric CO_2 concentration inside the spectrometer.

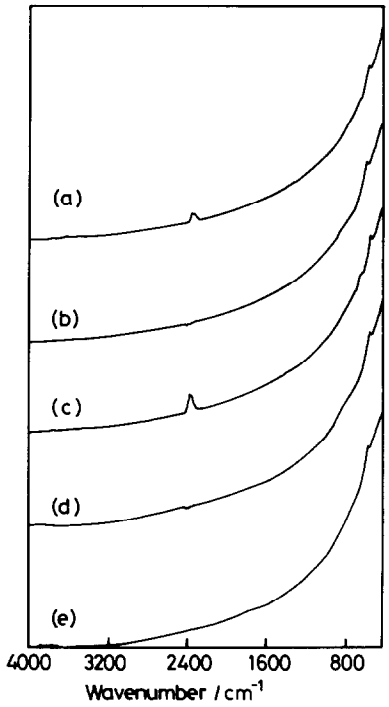

FIG. 5. IR reflectance of polycrystalline $YBa_2Cu_3O_7$ exposed to ambient atmosphere in London (a) as prepared (8–63%), (b) after 168 hr (6–51%), (c) after 552 hr (6–51%), (d) after 1447 hr (6–45%), (e) after 2400 hr (4–42%). Values in parentheses refer to the reflectance for each trace at 4000 and 400 cm^{-1}, respectively.

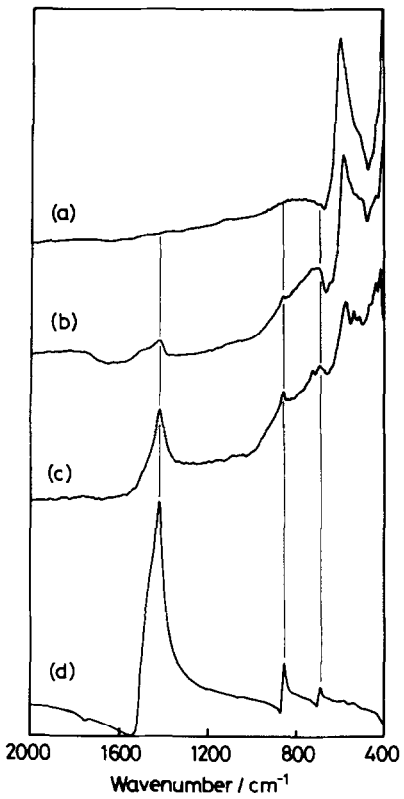

FIG. 6. IR reflectance of reduced polycrystalline $YBa_2Cu_3O_{7-\delta}$, $\delta \sim 1.0$, exposed to air saturated with water vapor (a) as prepared (2–17%), (b) after 1.5 hr (1–10%), (c) after 5 hr (0.4–2.9%). (d) IR reflectance of $BaCO_3$ (4–23%). Values in parentheses refer to the reflectance for each trace at 2000 and 400 cm^{-1}, respectively.

Figure 6 shows the results of degradation experiments carried out on the nonmetallic phase, nominally $YBa_2Cu_3O_6$. In this case, the spectrum of the as-prepared pellet shows strong Restrahl phonon features below 600 cm^{-1}, as in Fig. 1. On exposure to saturated water vapor, features associated with carbonate buildup are seen to appear on a time scale comparable with that for experiments on the metallic phase. Thus we can assert that the instability of the superconducting $YBa_2Cu_3O_7$ phase to surface degradation is in no way connected with the presence of the formal Cu^{III} valencies which are present in the metallic phase, but not in the nonmetallic phase $YBa_2Cu_3O_{7-\delta}$, $\delta > 0.5$.

While IR reflectance spectra in the region studied provide a useful indication of the progress of the surface reaction, we are unable from these spectra alone to observe the production of degradation products other than $BaCO_3$, or in fact to unambiguously assign the CO_3^{2-} species formed to $BaCO_3$. An experiment in which a CuO pellet was exposed to saturated water vapor for periods up to 168 hr showed the appearance of small features associated with carbonate buildup, and with water adsorption, indicating the formation of a small quantity of basic copper carbonate, perhaps via the scheme:

$$CuO + H_2O \rightarrow Cu(OH)_2 \quad (3)$$

$$2Cu(OH)_2 + CO_2 \rightarrow CuCO_3 \cdot Cu(OH)_2 + H_2O. \quad (4)$$

More specific information about the phases produced during the degradation reaction may be obtained from Raman spectra, where phases such as $BaCuO_2$, Y_2BaCuO_5, etc., may be identified from their distinct Raman phonon frequencies. Figure 7a shows the Raman spectrum of the green phase Y_2BaCuO_5, excited with the 488-nm (blue) line of an argon ion laser. This is compared with a similar spectrum of the metallic $YBa_2Cu_3O_7$ phase, previously exposed to water vapor saturated air for 280 hr. It is beyond the scope of this work to discuss in detail the assignments of the 54 Raman active lattice modes of the Y_2BaCuO_5 structure (*24*). However, the spectrum of the green phase shows a strong phonon feature at 603 cm^{-1} which must be associated with *M*–O stretching motion. In the spectrum of the degraded superconducting pellet, this feature is superimposed on a strong fluorescent background, but is nevertheless visible as a strong shoulder at 599 cm^{-1}. In addition, sharp features are

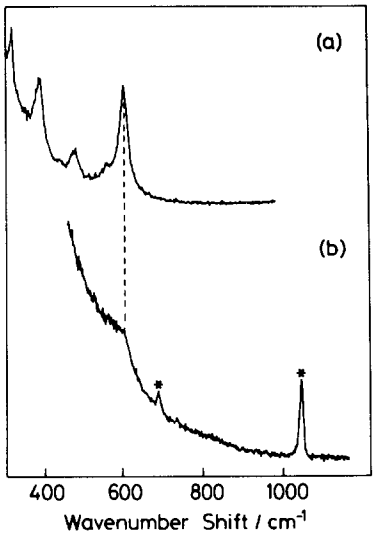

FIG. 7. (a) Raman spectrum of green Y_2BaCuO_5 excited with a 488-nm line of argon ion laser. (b) Raman spectrum of $YBa_2Cu_3O_7$ exposed to water vapor saturated air for 288 hr. Peaks marked with * are due to $BaCO_3$.

observed at 687 and 1055 cm^{-1}, which may be assigned, by comparison with similar spectra recorded from a $BaCO_3$ pellet, to the strong, sharp A_{1g} Raman active phonons of $BaCO_3$ (*22*). We note at this point that, as the carbonate series $CaCO_3$, $SrCO_3$, $BaCO_3$ all show very strong Raman active phonons, typically separated by approximately 10 wavenumbers from those of the other members (*23*), the technique is potentially very useful in similar experiments on the Bi–Sr–Ca–Cu–O superconducting phases, in differentiating between the production of $SrCO_3$ and $CaCO_3$.

Figure 8 shows XPS in the O : 1s and Ba : 3d regions for an as-prepared $YBa_2Cu_3O_7$ ceramic, which was directly transferred from the synthetic furnace, to the UHV spectrometer, with the minimum possible contact with the atmosphere. Spectra are recorded at normal (90°) emission and at 15° emission angle. Both O : 1s and Ba : 3d spectra are dominated by components to the high binding energy side of the peaks due to the 123 phase, which increase in relative intensity on going from normal to 15° emission angle. We thus associate these peaks with a contaminant overlayer. Uncleaned samples of this type were invariably contaminated with both adventitious hydrocarbon and carbonate species as evidenced by two-component C : 1s spectra. Again, the intensity of these features increased in grazing emission experiments. Because the Ba : 3d and O : 1s structures are clearly interrelated, we attribute at least

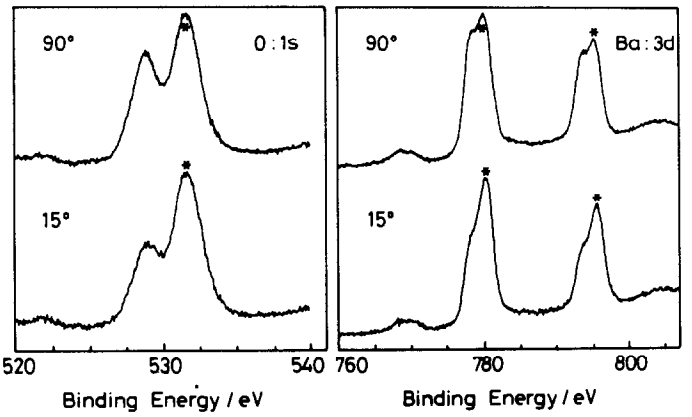

FIG. 8. Normal (90°) and 15° emission XPS of $YBa_2Cu_3O_7$ transferred to the XPS chamber straight out of the synthetic furnace. Peaks marked with * are due in part to $BaCO_3$ surface contamination.

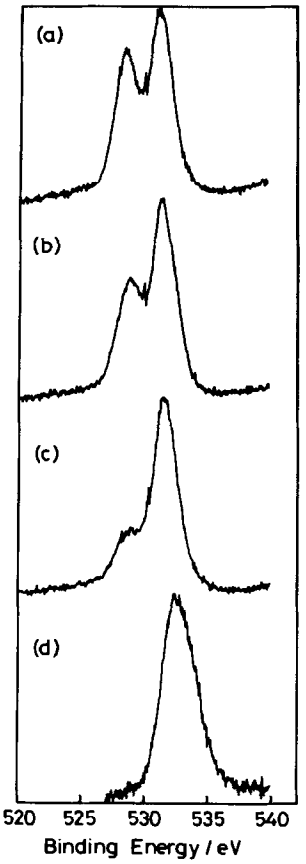

FIG. 9. O : 1s XPS of $YBa_2Cu_3O_7$ as a function of storage conditions (a) as in Fig. 9, (b) after 51 days storage in a plastic-cap-sealed glass bottle, (c) after 126 days storage as above, (d) after 100 days storage in open container in air.

part of the intensity in the high binding energy peaks to $BaCO_3$. It is clear that quite substantial contamination is present on an XPS depth scale, even in freshly prepared samples.

The intensity of the high binding energy features in the O : 1s and Ba : 3d regions were seen to increase regularly with the length of storage time after preparation. Figure 9 shows the O : 1s XPS of $YBa_2Cu_3O_7$ ceramics as a function of storage conditions. Of particular interest is the dramatic increase in contaminant buildup when the sample is stored in an open container in air (Fig. 9d). In this case, the carbonate oxygen peak totally obscures the signal from the underlying 123 phase. This may be contrasted with Fig. 9c, showing the spectrum from a sample stored for a longer period in a capped glass bottle, where the signal from the 123 phase may still be seen. The attenuation of the photoelectron flux on emergence from a sample is given by

$$I(x) = I_0(x)\exp(-x/\lambda), \qquad (5)$$

where $I(x)$ is the emerging flux of photoelectrons, and $I_0(x)$ is the flux of electrons of energy E originating at a depth x below the surface. Assuming a value for λ, the electron mean-free-path length of 15 Å (*25*), we may estimate the level of carbonate contamination by appropriate integration of Eq. (5). Assuming a carbonate overlayer of uniform thickness, we obtain estimates for the depth, d, of this layer of ~12, 17, 26, and 58 Å for the spectra of Figs. 9a–9d, respectively. Thus even the as-prepared pellet (Fig. 9a) shows a level of carbonate contamination sufficient to invalidate data from ultraviolet photoemission studies, where electron escape depths are of the order of 10 Å. Analysis of XPS peak intensities yields surface compositions for the samples represented in Fig. 9 which are enriched in Ba, C, and O, as expected; for the as-prepared pellet, we obtain a composition $Y_{0.91}Ba_{2.45}Cu_{2.64}O_{10.34}C(1)_{0.80}C(2)_{0.45}$, (where C(1) represents carbonate carbon and C(2) represents hydrocarbon), and for the sample stored for 100 days in air we obtain $Y_{0.75}Ba_{2.57}Cu_{2.68}O_{10.51}C(1)_{2.62}C(2)_{4.48}$.

After oxygen annealing inside the UHV spectrometer, the intensity of the carbonate C : 1s peak is dramatically reduced, and the feature due to hydrocarbon contamination is eliminated. It was in fact difficult to identify the weak residual peak due to carbonate in the raw spectra, as it lies below the $K\alpha_{3,4}$ satellite of the Y : 3p structure. However, after satellite stripping, the C : 1s/O : 1s intensity ratio in Al$K\alpha$ XPS was

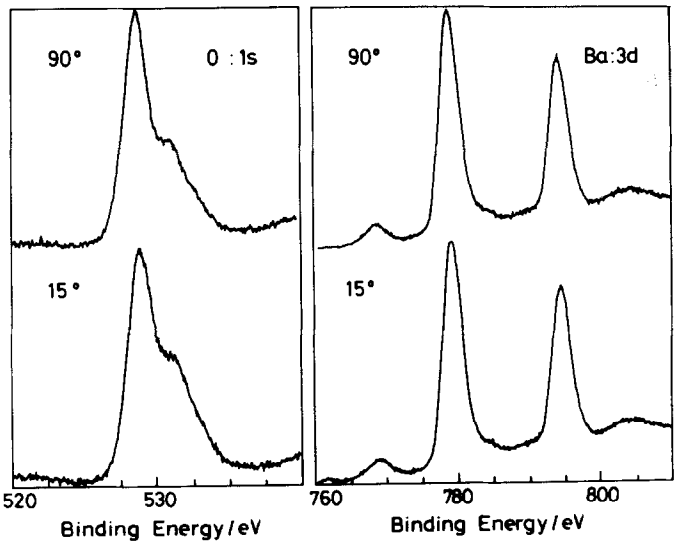

FIG. 10. XPS of $YBa_2Cu_3O_7$ after *in situ* cleaning in oxygen, revealing intrinsic peak shapes.

typically in the range 0.02 to 0.01, corresponding to residual carbonate coverage as low as 0.25 monolayer. As a guide, this is well below the level quoted for ceramic surfaces prepared by fracturing in UHV (*26*). Concomitant with the reduction in carbon signal, the high binding energy component of the Ba : 3d peaks disappears, as seen in Fig. 10. Spectral profiles are now invariant on going from normal to grazing emission angle. A high binding energy shoulder does remain in the O : 1s region with a small enhancement at shallow off-take angles. This shoulder is too strong to be associated with the low level of carbonate contamination. Comparable shoulders have been found in all previous experimental work where the O : 1s region was studied after some sample cleaning (*17, 27–30*). We thus believe the shoulder to be intrinsic to the 123 phase. Prior to *in situ* oxygen annealing, the sample which gave the spectra of Fig. 10 had been stored for a prolonged period in an open sample bottle in air, which resulted in the pronounced surface contamination of Fig. 9d. Thus our surface cleaning procedure may reverse even dramatic carbonate buildup, to leave samples suitable for surface-sensitive experiments, which show a surface elemental ratio not significantly different from the bulk nominal composition.

4. Conclusions

Our studies confirm that both metallic and nonmetallic phases of $YBa_2Cu_3O_{7-\delta}$ are subject to surface degradation via reaction with atmospheric CO_2. The reaction is strongly catalyzed by water vapor and shows a marked nonlinear dependence on $P(H_2O)$. This leads to the result that even modest precautions by way of sample storage (e.g., storage in stoppered sample bottles in a dessicator) may effectively stop appreciable degradation for periods of up to a year. We attribute the atmospheric instability of the superconductor to the very high thermodynamic stability of the $BaCO_3$ phase produced. Despite this, even the most serious surface contamination may be removed by *in situ* oxygen annealing inside a UHV spectrometer, to produce samples suitable for study by surface science tech-

niques (*13, 31, 32*), provided that the pellet retains its integrity.

Obviously, many factors, such as pellet morphology, temperature, CO_2 partial pressure, etc., will affect the rate of degradation of superconducting samples. We also do not suggest that the products of degradation necessarily build up in a laterally homogeneous way; in cases of severe surface reaction, $BaCO_3$ appears as white specks on the sample surface. We are, however, optimistic that surface reaction may be easily contained, and even under suitable circumstances reversed, to give the intrinsic surface of $YBa_2Cu_3O_7$ in thermodynamic equilibrium with the bulk.

Acknowledgments

We are grateful to R. Meisels, S. Bungre, and A. D. Caplin for resistivity measurements and to X. Turrillas for XRD work. The equipment used was funded by the SERC. W.R.F. is grateful to the Royal Society for the award of a 1983 University Research Fellowship.

References

1. J. G. Bednorz and K. A. Müller, *Z. Phys. B* **64,** 189 (1986).
2. M. K. Wu, J. R. Ashburn, C. T. Torng, P. H. Stor, R. L. Eng, L. Gao, Y. Q. Wang, Z. J. Huang, and C. W. Chu, *Phys. Rev. Lett.* **58,** 908 (1987).
3. R. M. Hazen, L. W. Finger, R. J. Angel, C. T. Prewitt, N. L. Ross, H. K. Mao, C. G. Hadidacos, P. H. Hor, R. L. Meng, and C. W. Chu, *Phys. Rev. B* **35,** 7328 (1987).
4. R. A. Camps, J. E. Evetts, B. A. Glowacki, S. B. Newcombe, R. E. Somekh, and W. M. Stobbs, *Nature (London)* **329,** 229 (1987).
5. D. Dinos, P. Chaudhari, J. Mannhart, and F. K. LeGoues, *Phys. Rev. Lett.* **61,** 219 (1988).
6. D. M. Kroeger, A. Choudhury, J. Brynestad, R. K. Williams, R. A. Padgett, and W. A. Coghlan, *J. Appl. Phys.* **64,** 331 (1988).
7. R. W. Vest, T. J. Fitzsimmons, J. Xu, A. Shaik, G. L. Liedl, A. I. Schindler, and J. M. Honig, *J. Solid State Chem.* **73,** 283 (1988).
8. J. R. Kirtley, R. T. Collins, Z. Schlesinger, W. J. Gallagher, R. L. Sandstrom, T. R. Dinger, and D. A. Chance, *Phys. Rev. B* **35,** 8846 (1987).
9. M. C. Gallagher, J. G. Adler, J. Jung, and J. P. Franck, *Phys. Rev. B* **37,** 7846 (1988).
10. P. Chaudhari, R. T. Collins, P. Freitas, R. J. Gambino, J. R. Kirtley, R. H. Koch, R. B. Laibowitz, F. K. LeGoues, T. R. McGuire, T. Penney, Z. Schlesinger, A. Segmüller, S. Foner, and E. J. McNiff, *Phys. Rev. B* **36,** 8903 (1988).
11. H. Rosen, E. M. Engler, T. C. Strand, V. Y. Lee, and D. Bethune, *Phys. Rev. B* **36,** 726 (1987).
12. I. Bozovic, D. Mitzi, M. Beasley, A. Kapitulnik, T. Geballe, S. Perkowitz, G. L. Carr, B. Lou, R. Sudharsanan, and S. S. Yom, *Phys. Rev. B* **36,** 4000 (1987).
13. W. R. Flavell and R. G. Egdell, *Supercond. Sci. Technol.* **1,** 118 (1988).
14. M. F. Yan, R. L. Barns, H. M. O'Brien, P. K. Gallagher, R. C. Sherwood, and S. Jin, *Appl. Phys. Lett.* **51,** 532 (1987).
15. I. Nakada, S. Sato, Y. Oda, and T. Kohara, *Japan. J. Appl. Phys.* **26,** L697 (1987).
16. K. Kitazawa, K. Kishio, T. Hasegawa, O. Nakamura, J. Shimogama, N. Sugii, A. Ohtomo, S. Yaegashi, and K. Fueki, *Japan. J. Appl. Phys.* **26,** L1979 (1987).
17. S. L. Qiu, M. W. Ruckman, N. B. Brookes, P. D. Johnson, J. Chen, C. L. Lin, B. Sinkovic, J. E. Crow, and C. S. Jee, *Phys. Rev. B* **37,** 3747 (1988).
18. R. L. Kurtz, R. Stockbauer, T. E. Madey, D. Mueller, A. Shih, and L. Toth, *Phys. Rev. B* **37,** 7936 (1988).
19. C. Kittel, "Introduction to Solid State Physics," Wiley, New York (1976).
20. T. R. Wonltungton, W. J. Gallagher, and T. R. Dinger, *Phys. Rev. Lett.* **59,** 1160 (1987).
21. G. Burns, F. H. Dacol, P. P. Freitas, W. Konig, and T. S. Plaskett, *Phys. Rev. B* **37,** 5171 (1988).
22. W. P. Griffith, *J. Chem. Soc. A,* 286 (1970).
23. Z. V. Popovic, C. Thomsen, M. Cardona, R. Liu, G. Stanisic, and O. Konig, *Solid State Commun.* **66,** 43 (1988).
24. W. B. White, *in* "The Infrared Spectra of Minerals" (V. C. Farmer, Ed.), Monograph 4, p. 241, The Mineralogical Society, London (1974).
25. M. P. Seah and W. A. Dench, *Surf. Interface Anal.* **1,** 2 (1979).
26. J. A. Yarmoff, D. R. Clarke, W. Drube, U. O. Karlsson, A. Taleb-Ibrahimi, and F. J. Himpsel, *Phys. Rev. B* **36,** 3967 (1987).
27. Z. Shen, J. W. Allen, J. J. Yeh, J. S. Kang, W. Ellis, W. Spicer, I. Lindau, M. B. Maple, Y. D. Dalichaoiuch, M. S. Torikachvili, J. Z. Sun, and T. H. Geballe, *Phys. Rev. B* **36,** 8414 (1987).

28. W. SCHINDLER, A. GRASSMAN, P. SCHMITT, J. SRÖBEL, H. NIEDERHOFFER, G. ADRIAN, G. SAEMANN-ISHCHENKO, AND H. ADRIAN, *Japan. J. Appl. Phys.* **26** (Suppl. 26-3), 1199 (1987).

29. P. STEINER, V. KINSINGER, I. SANDER, S. HÜFNER, AND C. POLITIS, *Z. Phys. B* **67,** 19 (1987).

30. T. KACHEL, P. SEN, B. DAUTH, AND M. CAMPAGNA, *Z. Phys. B* **70,** 137 (1988).

31. R. G. EGDELL AND W. R. FLAVELL, *Z. Phys. B,* in press.

32. W. R. FLAVELL AND R. G. EGDELL, *Phys. Rev. B* **39,** 231 (1989).